Transnational University Limburg is a unique collaboration of two universities in two countries: the University of Hasselt and Maastricht University.

UHASSELT
KNOWLEDGE IN ACTION

www.uhasselt.be
Universiteit Hasselt
Campus Hasselt:
Martelarenlaan 42 | 3500 Hasselt
Campus Diepenbeek:
Agoralaan Gebouw D | 3590 Diepenbeek

UHASSELT
KNOWLEDGE IN ACTION

Maastricht University

Faculty of Medicine and Life Sciences

School for Life Sciences

Master of Biomedical Sciences

Master's thesis

Optogenetic manipulation of dopaminergic neurons in a preclinical rodent model of Parkinson's disease

Nuran Caz

Thesis presented in fulfillment of the requirements for the degree of Master of Biomedical Sciences, specialization Molecular Mechanisms in Health and Disease

SUPERVISOR :
Prof. dr. Esther WOLFS

SUPERVISOR :
Asst. Prof. Andreas HEUER

MENTOR :
dr. Francesco GUBINELLI

2020
2021

Faculty of Medicine and Life Sciences

School for Life Sciences

Master of Biomedical Sciences

Master's thesis

Optogenetic manipulation of dopaminergic neurons in a preclinical rodent model of Parkinson's disease

Nuran Caz

Thesis presented in fulfillment of the requirements for the degree of Master of Biomedical Sciences, specialization Molecular Mechanisms in Health and Disease

SUPERVISOR :

Prof. dr. Esther WOLFS

SUPERVISOR :

Asst. Prof. Andreas HEUER

MENTOR :

dr. Francesco GUBINELLI

Optogenetic manipulation of dopaminergic neurons in a preclinical rodent model of Parkinson's disease

Nuran Caz[1,2], Francesco Gubinelli[1], Matilde Negrini[1], Tomas Björklund[3], Marcus Davidsson[3], Marco Ledri[4], Esther Wolfs[2,5] and Andreas Heuer[1]

[1]Behavioural Neuroscience Laboratory, Department of Experimental Medical Sciences, Lund University, Lund, Sweden
[2]Faculty of Medicine and Life Sciences, Hasselt University, Diepenbeek, Belgium
[3]Molecular Neuromodulation, Department of Experimental Medical Sciences, Lund University, Lund, Sweden
[4]Epilepsy Center, Department of Clinical Sciences, Faculty of Medicine, Lund University, Lund, Sweden
[5]Department of Cardio and Organ Systems, Biomedical Research Institute, Hasselt University, Diepenbeek, Belgium.

To whom correspondence should be addressed: Andreas Heuer, Tel: +46 70 883 62 98; Email: andreas.heuer@med.lu.se

Keywords: Parkinson's disease; optogenetics; dopaminergic neurons; electrochemistry; Channelrhodopsin

ABSTRACT

Parkinson's disease (PD) is a neurological disease characterised by progressive loss of dopamine-producing neurons, giving rise to motor and cognitive symptoms. Although intracerebral transplantation of dopamine-producing cells has been shown to be a feasible approach in preclinical and clinical studies, the working of a transplant is inferred by correlations rather than causative studies. This project aims to demonstrate the functionality of transplanted neurons by selectively and reversibly perturbating the cell activity of engrafted neurons using optogenetics. First, we identified the optimal optogenetic-stimulation parameters via *in vivo* electrochemical detection of dopamine release. Based on these results, we investigated the function of dopaminergic rat fetal grafts in rats that were rendered hemiparkinsonian via unilateral 6-hydroxydopamine injections, followed by intrastriatal engraftment. Subsequently, the graft was transduced with a Cre-inducible adeno-associated viral vector to selectively express Channelrhodopsin-2 in engrafted dopamine cells. Behavioural deficits and improvements were assessed through the drug-induced rotation test and the cylinder test. After graft maturation, selective graft functionality was examined through electrophysiological and electrochemical optogenetic manipulation. Results indicate that higher laser intensity and stimulation duration result in increasing release trends of dopamine. Moreover, the PD-lesioned rats displayed an impaired behavioural motor activity followed by behavioural improvements post-transplantation. Intra- and extracellular measurements of the graft in combination with optogenetics further supported the graft survival and functioning. This study provides evidence on the ability of optogenetics to selectively activate the opsin-expressing dopaminergic transplants. Unravelling the integration and functionality of transplants using optogenetics will strengthen the potential of cell replacement therapy for PD.

INTRODUCTION

Parkinson's disease (PD) is a progressive neurodegenerative disorder affecting over 10 million people worldwide. Age is known to be the greatest risk factor for this condition, with a mean age of onset of approximately 50 to 60 years (1). The underlying pathological cause is the gradual loss of dopaminergic neurons in a pathway involved in controlling and facilitating movement. This pathway, called the nigrostriatal system, originates from the substantia nigra (SN) pars compacta in the midbrain and provides dopaminergic innervation to the striatum in the forebrain. Progressive degeneration of the neurons

in the nigrostriatal pathway leads to dopamine deficiency, giving rise to characteristic PD symptoms including bradykinesia, resting tremor, akinesia, and postural impairment. Many patients also experience non-motor deficits such as sleep disruptions, depression, constipation, and difficulties with swallowing or speech. All these symptoms lead to a decreased quality of life, emphasising the need for therapies (2, 3).

Despite that there is no definitive cure for PD, many of the current treatments focus on maintaining the symptoms by increasing or surrogating dopamine in the brain. Dopamine itself cannot be used as a direct therapeutic for PD since it does not cross the blood-brain barrier (4). Contrarily, levodopa is a natural chemical that enters the brain and gets converted into dopamine by the remaining neurons resulting in significant improvements of the symptoms. Unfortunately, these effects will not be enduring as the neurons that take up this molecule degenerate over time. Although levodopa is the gold standard for treating PD, it will eventually lead to off-target side effects such as dyskinesias (5). Efforts are also being made to provide more supportive therapies for PD patients; however, these aim to ameliorate the quality of life and maintain the symptoms rather than cure the disease. Advanced patients in which conservative therapies show unstable responses can be offered deep brain stimulation (DBS). This includes the surgical implantation of electrodes that are able to send electrical pulses in specific parts of the brain (6). PD patients have experienced recognisable long-term benefits from DBS, but these are again limited since it does not halt the disease progression (7). The off-target effects of current therapies, together with the progressive degeneration of neurons are requiring a different approach in substituting dopamine more locally in the affected brain area (8).

Degeneration of the dopaminergic neurons makes PD particularly suitable for cell replacement therapies (9). It has already been reported that transplantation of primary fetal tissue-derived dopamine neurons into the lesioned striatum induced functional recovery in preclinical rodent models of PD as well as in clinical trials (10-13). Among others, these grafts demonstrated expression of dopamine neuron-specific markers and restoration of characteristic functions such as dopamine release. Transplantation with human embryonic stem cells in rats showed a long-time survival of the cells and motor recovery, indicating its therapeutic application towards the clinic. To date, several clinical trials using cell replacement therapy have already been conducted, showing the success of this approach, at least in a subset of patients (14). Yet, some questions regarding the correlation between the graft-induced recovery and the transplanted cells in both rodent and human studies remain unanswered. Current assessment of graft function is mainly based on correlating behavioural evaluation with post-mortem histopathology. Previous studies demonstrated the graft function merely indirectly through reinstating the behavioural deficits in animals when the entire transplant was physically removed or when the dopaminergic grafts were selectively killed (15, 16). Furthermore, Steinbeck et al. showed that silencing the graft activity re-introduced the motor deficits in mice that had recovered from lesion-induced Parkinson-like impairments (17). The specific role of the grafted neurons cannot be identified through complete inhibition of the neurons from the transplant, indicating the importance of a method to validate the functional integration of the grafts into the neuronal circuits.

To gain more insights into the causal relationship between graft function and behavioural response, optogenetics can be implemented. This method uses optical stimulation and genetic modifications to selectively perturbate the cellular activity of engrafted neurons (18). The reversible manipulation of genetically defined neurons allows optogenetics to interconnect neuronal activity with animal behaviour. Several endeavours have already been successfully made to elucidate the neural circuits underlying mood disorders, addiction, and PD (18-20). To apply this in PD-lesioned rats, a microbial photosensitive protein called Channelrhodopsin-2 (ChR2) needs to be introduced into genetically modified target cells. In this study, the grafts are derived from transgenic tyrosine hydroxylase-Cre (TH:Cre^{tm1sage}) rat embryos, which are characterised by the expression of Cre-recombinase under the control of the endogenous TH promoter for dopaminergic neurons. Subsequently, Cre-inducible viral vectors expressing the opsin are delivered into these cells,

enabling ChR2 expression in dopamine neurons only (21). Once expressed, ChR2s are able to be activated through blue-light (peak 470 nm) illumination, resulting in depolarisation and, therefore, activation of the neurons due to passage of cations (18, 20, 22, 23).

Before applying optogenetics in a freely-moving setting to demonstrate an altered behaviour, it is crucial to validate the functioning of ChR2 in a surviving graft. So rather than removing the transplants and reinstating the motor deficits, this project aims to combine optogenetics with electrochemical and electrophysiological detection methods to determine the graft functionality in a unilateral 6-hydroxydopamine (6-OHDA)-lesioned PD rat. Identifying the graft functionality using optogenetics will bring us one step closer to better understanding the mechanism of brain recovery and confirm the efficacy of cell replacement therapy as a promising therapeutic intervention for PD.

EXPERIMENTAL PROCEDURES

Research animals

Female adult (200-250 g) Sprague-Dawley, wild-type (Charles River) and TH:Cre^{tm1sage} (in house breeding) rats were housed in standard laboratory cages with free access to food and water under a 12:12 h dark-light cycle in a temperature-controlled room. All experimental procedures were approved by the Ethical Committee for Use of Laboratory Animals in the Lund-Malmö region.

AAV vector production

Double-floxed Inverted Orientation Adeno-associated Virus-6 (DIO-AAV-6) vectors containing the EF-1a-ChR2-EYFP construct were produced by dual-plasmid, calcium precipitation mediated transient transfection of HEK-293 cells and purified by iodixanol gradient centrifugation and anion exchange chromatography as described previously (24). Using the woodchuck hepatitis virus posttranscriptional regulatory element (WPRE), the sequences were 3' untranslated region flanked and terminated with an SV40 derived poly-adenylationsequence. Viral titres were quantified using ddPCR, yielding a titre of 6.5E13 gc/ml, with primers against the AAV inverted terminal repeat sequences. This was then diluted to a working titre of 1E12 gc/ml.

Preparation of fetal dopaminergic cells

Dopaminergic rat progenitors cells were obtained as previously described (25, 26). Briefly, on embryonic day 14, TH:Cre heterozygous embryos were taken out from the embryonic sac. Following, the ventral mesencephalon of each fetus was carefully dissected and transferred into ice-cold DMEM/F12 media. Afterwards, the fetal tissue was incubated with 0.1% trypsin and 0.05% DNAse in HBSS for 20 min at 37°C. The cells were mechanically dissociated and engrafted into the striatum of 6-OHDA lesioned wild type Sprague Dawley rats (2 µl of 10E4 viable cells/µl, a total of 200 000 cells). A detailed description of the protocol is provided in the supplementary methods.

Stereotaxic surgery

Rats were deeply anaesthetised prior to all surgical procedures using gaseous isoflurane (3-4 %) and placed into the stereotactic frame. A small hole was then drilled through the skull. A pulled glass capillary was attached to a 10 µl Hamilton syringe and connected to an automated infusion pump system to perform the injections. For the unilateral lesions, 3 µl of 6-OHDA (Cl-salt, Sigma-Aldrich) was infused into the medial forebrain bundle (MFB) according to the following coordinates (in mm, from Bregma): AP= -4.0; ML = -1.3; DV= -7.0 with an infusion rate of 0.5 µl/min. For the engraftment, fetal dopaminergic progenitors were infused into the striatum at the following coordinates: AP= +1.0; ML= -2.6; DV= -4.0, with a rate of 0.5 µl/min and an injection volume of 2 µl. AAV-6 viral vectors were infused into the striatum with a volume of 2 µl at a rate of 0.5 µl/min in the same site of the engraftment: AP= +1.0; ML= -2.6; DV= -4.0. Following all the infusions, the glass capillary was left in position for three min before being gently retracted.

Tissue preparation

Following chronoamperometry recordings, animals were sacrificed by pentobarbital overdose and trans-cardially perfused. The brains were collected and post-fixed for 24 h in ice-cold PFA and eventually stored in 25% buffered sucrose as cryoprotectant for at least 24 h. The brains were sliced into 40µm coronal sections using a sliding microtome (HM 450, Thermo Scientific) and stored in antifreeze solution at −20°C until further processing. Animals used for patch clamp

recordings were decapitated, after which the brain was harvested and transferred to a cutting chamber with sucrose-based solution maintained at 2–4°C while constantly oxygenated with carbogen (95% O2/5% CO2). Using a vibrating microtome (VT1200S, Leica Microsystems), the brain was sliced with a thickness of 300 µm and immediately transferred to an incubation chamber containing sucrose-based solution constantly oxygenated with carbogen (95% O2/5% CO2) and maintained at 34°C in a water bath. Slices rested for 30 min before being transferred to room temperature and processed for electrophysiology.

Immunohistochemistry

Immunohistochemical stainings were performed as previously reported (27). A detailed description of the protocol as well as an overview of the used primary and secondary antibody pairs and concentrations can be found in supplementary methods (**Suppl. Table 1**). The primary antibodies that were utilised for DAB immunohistochemistry were anti-GFP and anti-TH. The used biotinylated secondary antibodies were respectively anti-chicken and anti-rabbit and were amplified by the Vectorlabs avidin-biotin complex (ABC) kit. For immunofluorescence, we used the primary anti-GFP, anti-TH, and anti-Cre antibodies with their respectively corresponding Alexa-conjugated secondary antibodies: anti-chicken (Alexa 488), anti-rabbit (Alexa 568), and anti-mouse (Alexa 647). For staining against biocytin, we utilised the Alexa 647-conjugated streptavidin (1:1000, Thermofisher).

Behaviour tests

Drug-induced rotation test

The drug-induced rotation test was used to assess the efficacy of the 6-OHDA lesion and the grafted dopaminergic progenitors. Rats were placed into an automated rotameter bowl and recorded using a rotation software (AccuScan Instruments Inc.). After 10 min of habituation, rats were injected with 2.5 mg/kg *d*-amphetamine (i.p.) and recorded for 90 min. Upon 0.05 mg/kg apomorphine (s.c.) injections, rats were recorded for a total of 60 min.

Cylinder test

To determine the asymmetric forelimb behaviour, rats were placed in a glass cylinder (20 cm in diameter) and were recorded with a digital video camera. To clearly visualise the animals from all angles, two perpendicular mirrors were placed behind the cylinder. We recorded the animals for 5 min or for at least 20 touches between the paw and the walls of the glass cylinder. Animals were scored according to the percentage of ipsilateral (right) or contralateral (left) touches out of the number of total touches.

***In vivo* electrochemical recordings**

Electrochemistry was performed as previously described (26). In brief, calibrated Nafion-coated carbon fibre electrodes were mounted together with a glass micropipette and the optical fibre for light stimulation. The assembly was inserted into the brain and three successive chronoamperometric recordings for dopamine were performed for each stimulation parameter (**Table 1**). A detailed description of the protocol is provided in supplementary methods

Whole-cell patch clamp electrophysiology

Individual slices were placed in a dual-flow recording chamber with carbogenated artificial cerebrospinal fluid (aCSF) at a maintained temperature of 32°C-34°C. Recording pipettes were filled with the patching solution and the visualised GFP-positive cells were approached. The firing activity of the cells was measured following either current injections or light stimulation pulses. Prior to gently retracting the pipette, biocytin was allowed to diffuse in the cell for 10 min. A detailed overview of the procedure is provided in the supplementary methods.

Table 1 Stimulation parameters for optogenetics-combined chronoamperometry recordings

Laser intensity (mW)	Stimulation duration (sec)	Dorsoventral position (relative to bregma)	Light frequency (Hz)
0.625	5	-1.0	Constant
1.25	30	-3.5	20 Hz
2.5	60	-4.5	40 Hz
5	120	-5.5	

Imaging

Brightfield images were captured using a Leica DMI8 inverted microscope. Fluorescent images were taken by either the same microscope or using a Leica SP8 laser scanning confocal microscope with a 488 nm, 568 nm, and 647 nm solid-state laser activation in sequential mode and with a pinhole of 1AU.

Statistical analysis

Data were statistically analysed using GraphPad Prism v6 (GraphPad Software). Normal distribution was tested using the Shapiro-Wilk normality test. Data sets with > two groups with normal distribution were analysed with repeated measures ANOVA and not normally distributed data sets were analysed with the Friedman test followed by the post-hoc Dunn's test. Two-group data sets with normal distribution were analysed using a one-tailed paired student t-test and not normally distributed data sets were analysed using a Wilcoxon signed-rank test. Statistical significance is presented as * $p < 0.05$,** $p < 0.01$ in all figures. All data are reported as mean ± standard error of the mean (SEM).

RESULTS

AAV containing ChR2 is expressed in target TH:Cre cells

Optogenetics is an emerging yet recent technique in the field of neuroscience, making it crucial to optimise its application in *in vivo* models. To investigate the parameters in which the optogenetic stimulation would be the most optimal, we injected TH:Cre rats in the SN (right) with an AAV containing ChR2-EYFP (**Fig. 1A-B**). After a waiting period of four weeks to enable transgene expression, extracellular dopamine levels were recorded by chronoamperometry upon light stimulation (**Fig. 1A**). Firstly, the ChR2 expression in TH:Cre-positive cells was confirmed by performing immunohistochemical staining against GFP in nigral and striatal sections (**Fig. 1C**). GFP was expressed in the injected hemisphere only and cells were clearly visualised at the injection site in the SN (**Fig. 1C^{I}**). Furthermore, co-localisation of GFP-positive cells with TH and Cre indicated that the opsin protein was only expressed in TH-positive cells in the presence of Cre recombinase (**Fig. 1D-D^{III}**). Overall, these results illustrate that the AAV-ChR2 is selectively expressed in the TH:Cre cells and as a result, they are suited for the application of optogenetics.

Optimising optogenetic stimulation parameters through chronoamperometric dopamine detection

After validating ChR2 expression in the target cells, *in vivo* electrochemical measurements were performed in the striatum of injected TH:Cre rats to identify the light-driven dopamine release in real-time. An assembly including a KCl-filled glass capillary, a Nafion-coated carbon fibre electrode, and an optical fibre was constructed and inserted into the centre of the dorsal striatum, in the caudate putamen, of the injected hemisphere (**Fig. 2B**). Dopamine release was evoked by either light stimulation from the optical fibre or a fixed amount (about 100 nl) of pressure-induced KCl injection. Several parameters were tested including laser intensity, frequency, and duration at different stereotactic DV coordinates to define the optimal stimulation conditions (**Table 1**). The different depth profiles were used as an internal control to ensure that dopamine is only released in the striatum. **Fig. 2A** represents an individual trace at position -3.5, which is the target structure to where the nigral dopaminergic cell bodies project, for respectively 0.625 (*red*), 1.25 (*blue*), and 2.5 mW (*green*) during 5, 30, 60, and 120 s for constant light stimulation. The detected dopamine concentrations show an overall increasing trend upon higher laser intensity as well as longer stimulation duration. Moreover, all the individual parameters were tested in several rats to determine the maximal extracellular dopamine concentration (peak amplitude) and the total amount of dopamine available to act on the postsynaptic receptors (area under the curve (AUC).

We demonstrated that the maximum reached dopamine concentration was approximately 0.5 µM for a laser intensity of 0.625 mW (**Fig. 2C**). Whereas we expected to see a higher dopamine concentration in the -3.5 position, the difference among the several depth profiles was not remarkable for this laser intensity, nor was the duration (**Fig. 2C**). Similarly, the depth profiles did not show differences in the total amount of dopamine available (**Fig. 2D**). Furthermore, the highest dopamine concentration for a 1.25 mW

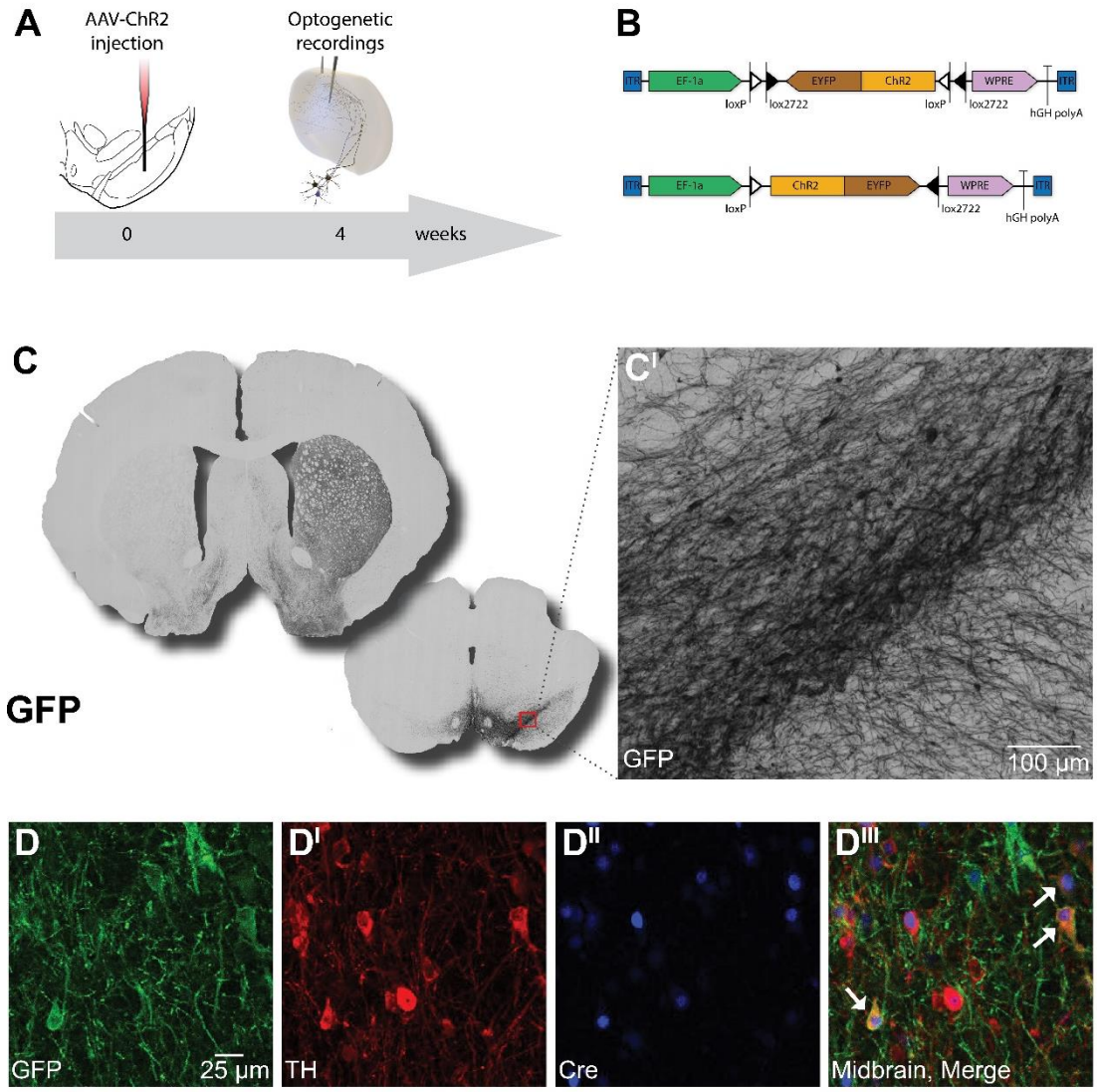

Figure 1 AAV-ChR2 expression is selective for TH:Cre cells. (**A**) Experimental timeline illustrating the time points of virus injection into the midbrain of TH:Cre rats and optogenetic recordings using electrochemistry. (**B**) Schematic of the viral construct including ITR, the EF-1a promoter, an EYFP-ChR2 fused transgene surrounded by a pair of LoxP and Lox2722 sites, a WPRE, and a hGH polyA in the inactive double floxed inverted orientation (*top*) and in the active fixed orientation of the transgene (*bottom*). (**C**) Representation of a DAB-stained coronal striatal and midbrain section labelled against ChR2 (GFP) with (**C^{I}**) higher magnification of ChR2 (GFP)-expressing cells in the substantia nigra. (**D-D^{III}**) Representative images of immunofluorescent labelling of ChR2 (GFP), dopaminergic neurons (TH), and Cre-recombinase (Cre) in midbrain sections. White arrows indicate complete co-localization. AAV: adeno-associated virus; ITR: inverted terminal repeats; EF-1a: elongation factor 1 alpha; EYFP: enhanced yellow fluorescent protein; ChR2: channelrhodopsin-2; WPRE: woodchuck hepatitis virus post-transcriptional regulatory element; hGH polyA: human growth hormone polyadenylation; GFP: green fluorescent protein; TH: tyrosine hydroxylase.

stimulus was around 1 µM (**Fig. 2E**). This was perceived for stimulation of 60 s at -3.5. Contrary to the 0.625 mW stimulation, there was a reduced release pattern in structures other than the target structure, with a significantly higher release in the striatum when compared to -5.5. The total amount of released dopamine (AUC) obtained by 1.25 mW stimulation indicated the same release pattern as the

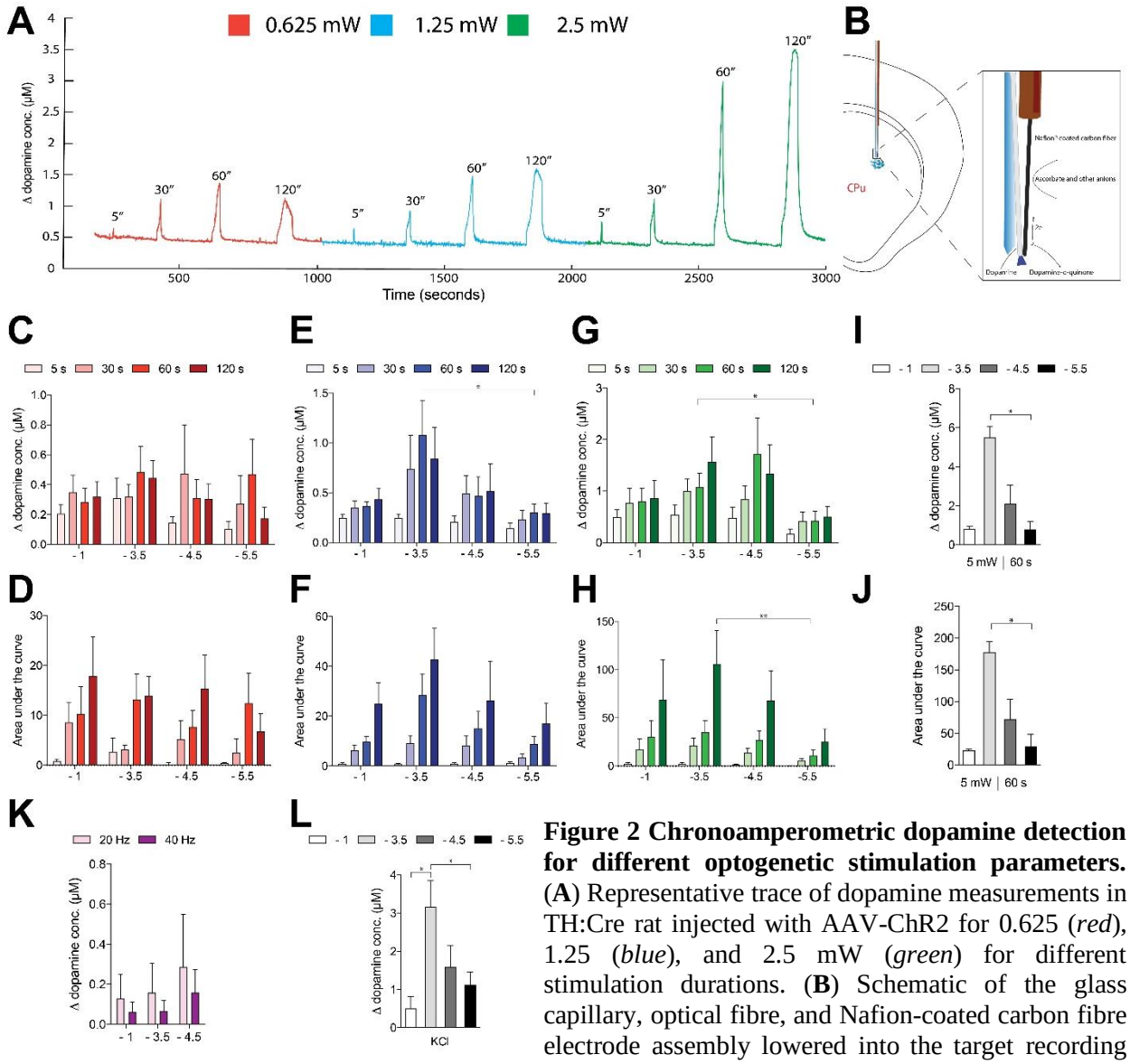

Figure 2 Chronoamperometric dopamine detection for different optogenetic stimulation parameters. (**A**) Representative trace of dopamine measurements in TH:Cre rat injected with AAV-ChR2 for 0.625 (*red*), 1.25 (*blue*), and 2.5 mW (*green*) for different stimulation durations. (**B**) Schematic of the glass capillary, optical fibre, and Nafion-coated carbon fibre electrode assembly lowered into the target recording position in the striatum. Detected dopamine concentrations (µM) and area under the curve for a constant laser power of respectively (**C-D**) 0.625 (*red*), (**E-F**) 1.25 (*blue*), (**G-H**) 2.5 (*green*), and (**I-J**) 5 mW (*grey*) stimulation for indicated durations and dorsoventral positions. Detected dopamine concentrations (µM) for (**K**) different frequencies (*pink*) and (**L**) KCl injections (*grey*) in indicated dorsoventral positions (n=4-6). Data are represented as mean ± SEM. *$p < 0.05$, **$p < 0.01$. CPu: caudate putamen.

dopamine concentrations (**Fig. 2F**). A laser power of 2.5 mW yielded a maximum dopamine concentration of around 1.7 µM, mainly in the -3.5 and -4.5 position (**Fig. 2G**). Also with this laser power, dopamine release was significantly higher in the striatum in comparison to -5.5. The AUC for a laser power of 2.5 mW also suggested the highest amount of dopamine in -3.5 (**Fig. 2H**). Despite no differences in duration for the dopamine concentrations, comparison of the AUC for the duration parameters revealed a significantly higher amount of dopamine for 120 s over 5 s stimuli (not shown on the figure, $p < 0.05$) for 0.625, 1.25, and 2.5 mW.

Besides these parameters, we also evaluated the dopamine release for a 5 mW laser intensity. Since this might damage the tissue due to excessive heat, it was only tested for 60 s in all the positions, resulting in the highest dopamine concentration and

amount of dopamine in the striatum, with a significant increase when compared to -5.5 (**Fig. 2I-J**). In addition, the response to pulsed illumination with a frequency of either 20 or 40 Hz was also assessed. Due to a limited number of animals, we were only able to test these parameters for a laser power of 2.5 mW during 60 s as they seemed to be the most promising stimuli. Although 20 Hz light pulses showed a higher dopamine concentration when compared to 40 Hz, the release was rather deficient (**Fig. 2K**). Lastly, the detected peaks were validated using KCl injections to trigger the release of dopamine. The latter provoked the cells to release dopamine, with significantly higher concentrations in the striatum over the -1 and -5.5 positions (**Fig. 2L**). To conclude, laser intensities of 0.625 mW and 5 mW were respectively too weak or too powerful to induce a dopamine release similar to KCl. A power of 1.25 and 2.5 mW were more likely to show a similar effect in the striatal cells. When looking at the duration, 5 s and 30 s were not long enough to provoke the release of all the available dopamine, yet, the maximum peak can possibly already be attained after 60 s. Besides, constant light results in better stimulation when compared to pulsed light.

6-OHDA lesioned rats demonstrate expression of AAV-ChR2 in a surviving graft

To investigate the graft functionality in PD-induced rats using optogenetics, we injected the neurotoxin 6-OHDA into the MFB to deplete the dopamine unilaterally (**Fig. 3A**). Following the induction of the disease model, the rats received a transplantation of fetal dopaminergic progenitor cells (E14) derived from TH:Cre rats in the depleted striatum. After allowing maturation of the cells, the viral transduction of ChR2-GFP took place to finally enable the optogenetic manipulation of the grafted cells (**Fig. 3A-B**). Immunohistochemical analysis for dopaminergic neurons (TH) revealed that 6-OHDA administration led to a complete depletion of dopamine in the injected hemisphere (**Fig. 3C**). In addition, we observed that the engrafted cells matured and survived in the striatum (**Fig. 3C^{I}**). To evaluate the viral expression, we performed a fluorescent staining against GFP and TH. In the injection site, we observed a GFP expression with a clear fibre extension as well as expression of TH-positive cells (**Fig. 3D-D^{I}, E-E^{I}**). The latter was co-localised with the GFP-positive cells in the graft (**Fig. 3D^{II}, E^{II}**). These data demonstrate that dopamine was thoroughly depleted due to a successful lesion and that engrafted dopamine cells survived and expressed ChR2.

Behavioural improvements in 6-OHDA rats after transplantation suggest a graft-induced motor recovery

In order to verify the graft survival with motor recovery, several behavioural tests were performed. The principal test was the drug-induced rotation test with either amphetamine or apomorphine. Amphetamine acts as a presynaptic dopamine transporter inhibitor and allows the stimulation of dopamine release while blocking the dopamine reuptake (28). This leads to rotations in the direction ipsilateral to the 6-OHDA lesion. Apomorphine acts as a postsynaptic dopamine agonist and induces rotations in the contralateral direction via stimulation of hypersensitive postsynaptic receptors (28). Rats displaying a rotation rate higher than 5 rotations per minute (rpm) for the amphetamine test indicated a successful lesion and were further included in the behavioural analysis (n=6) (**Fig. 3F**) (29). The number of rotations decreased after engraftment and is indicative of behavioural recovery. To gain more accurate understanding on the rotational behaviour of the rats over the 90 min testing period, we delved into the complete time course divided in three intervals of 30 min. Analysis shows that there is a shift from high ipsilateral to contralateral rotations in respectively lesioned and transplanted rats with significant improvements in the rpm for the first two intervals (**Fig. 3I**). After 60 min, the animals reach the baseline at both lesion and transplantation time-points due to the diminished effect of amphetamine in the SN. On the other hand, the same behavioural improvements could not be seen with the apomorphine test. The rats rotated contralaterally after the lesion, which validated its success but showed a similar response after transplantation (**Fig. 3G**). The apomorphine time course also illustrated that the animals were rotating contralaterally, yet, there was no observed difference post-transplantation (**Fig. 3J**). Therefore, the graft-induced improvements in the lesioned rats were confirmed by performing the amphetamine test again using different doses and over a time period of 300 min to only stimulate the

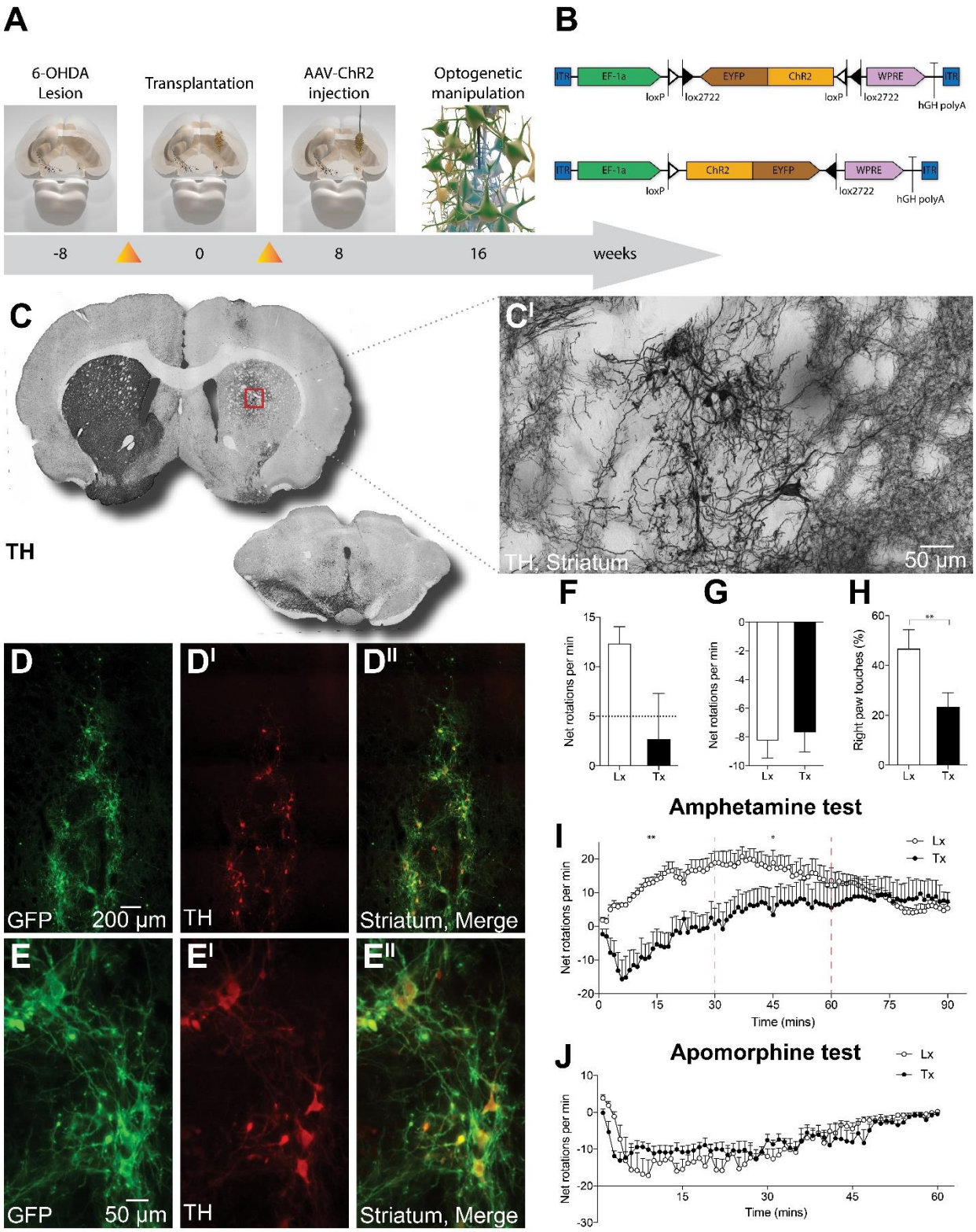

grafted hemisphere. Rats that showed the best improvements of the deficits according to the previously performed amphetamine test were selected and evaluated for rotational behaviour after administration of saline, 0.625, 1.25 or 2.5 mg/kg amphetamine (**Suppl. Fig. 1**). Whereas the rats showed a stable response to a control injection of saline, contralateral rotational behaviour was

Figure 3 Mature TH:Cre transplanted cells ameliorate 6-OHDA-induced impairments. (**A**) Experimental timeline showing main procedures with behavioural assessment (*orange triangles*) and optogenetic manipulation. (**B**) Schematic of the viral construct including ITR, the EF-1a promoter, an EYFP-ChR2 fused transgene surrounded by a pair of LoxP and Lox2722 sites, a WPRE, and a hGH polyA in the inactive double floxed inverted orientation (*top*) and in the active fixed orientation of the transgene (*bottom*). (**C**) Representation of a DAB-stained coronal striatal and midbrain section against dopaminergic neurons (TH) with (**C^{I}**) higher magnification of matured dopaminergic neurons in the striatum. (**D-E^{II}**) Representative images and higher magnification of immunofluorescent staining against ChR2 (GFP) and dopaminergic neurons (TH) in the striatum. (**F**) Amphetamine-induced rotation test with (**I**) 90 min time course divided into three 30 min intervals (*dotted red line*), (**G**) apomorphine-induced rotation test with (**J**) 60 min time course and (**H**) cylinder test with data expressed as the percentage of right paw touches over the left paw, after 6-OHDA lesioning and transplantation surgeries (n=6). Data are represented as mean ± SEM. *p<0.05 **p <0.01. 6-OHDA: 6-hydroxydopamine; AAV: adeno-associated virus; ChR2: channelrhodopsin-2; ITR: inverted terminal repeats; EF-1a: elongation factor 1 alpha; EYFP: enhanced yellow fluorescent protein; WPRE: woodchuck hepatitis virus post-transcriptional regulatory element; hGH polyA: human growth hormone polyadenylation; TH: tyrosine hydroxylase; GFP: green fluorescent protein. Lx: lesion; Tx: transplantation.

already triggered with the lowest dose of amphetamine. Over time, the number of net rpm was gradually returning to a baseline response. The 1.25 mg/kg administration triggered a similar response but showed a peak of 0 rpm between min 50 and 100. The 2.5 mg/kg amphetamine injection started with a high number of contralateral rotations but reached the highest peak of net ipsilateral rotations among all doses. Lastly, impairments in the forelimb use were assessed using the cylinder test and data was expressed as the percentage of right paw touches over the left paw (**Fig. 3H**). Post-lesioning, the rats were more likely (47%) to use their right paw over the left. However, after transplantation, this percentage was significantly decreased and rats were using their left paws more frequently. To conclude, the rats showed an impaired behavioural output after the PD lesion followed by a recovery post-transplantation.

Optogenetics enables manipulation of ChR2-expressing grafts

To finally modulate the grafted cells using optogenetics and determine the functionality, we performed both electrophysiological and electrochemical detection measurements. For whole-cell patch clamp recordings of the ChR2-GFP-expressing cells, we first examined the firing of action potentials in current clamp mode. Starting from negative current injections of 25 pA, we detected small capacitive currents (**Fig. 4A**). Following, +25 pA and +75 pA current injections resulted in the firing of action potentials once the threshold of depolarisation was reached. Furthermore, constant light stimulation of 500 ms revealed one strong action potential, whereas the cell fired several action potentials on pulsed light stimulation (**Fig. 4B-D**). We also studied the electrophysiological behaviour of the cell by recording it 30 s before and during light stimulation in current clamp mode (**Fig. 4E**). Pre-light, the cell showed a maintained resting potential with some spontaneous firing of action potentials. During light stimulation, there was no noticeable upregulation of action potentials; however, the light triggered a shift towards a depolarising graded potential and a fast spiking response. The latter indicates an increased influx of cations due to interactivity with surrounding excitatory neurons. Imaging of biocytin that was released into the cells during patch clamp recordings, validated that the patch was performed on the transplanted neurons (**Fig. 4F-G**). This also demonstrates the survival and maturation of grafted cells in the striatum by visualising the axonal arborisation (**Fig. 4G^{I}**). In addition, the ability of the grafted cells to release dopamine was identified using chronoamperometry. A representative trace of dopamine detection upon local laser stimulation on the graft displays that the cells release dopamine, only during illumination, followed by reuptake of dopamine (**Fig. 4H**). To summarise, optogenetic manipulation of the graft provoked the firing of action potentials and release of dopamine.

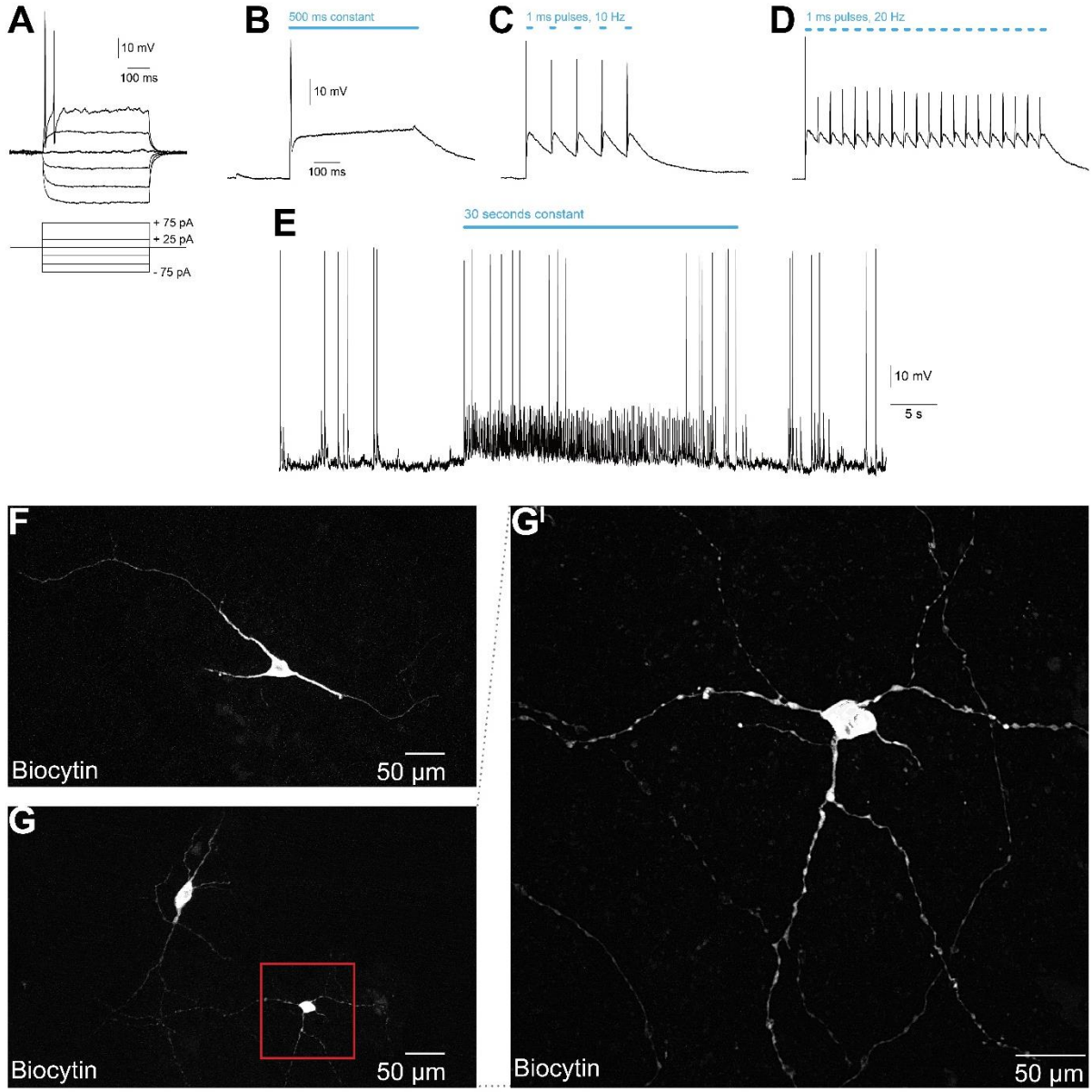

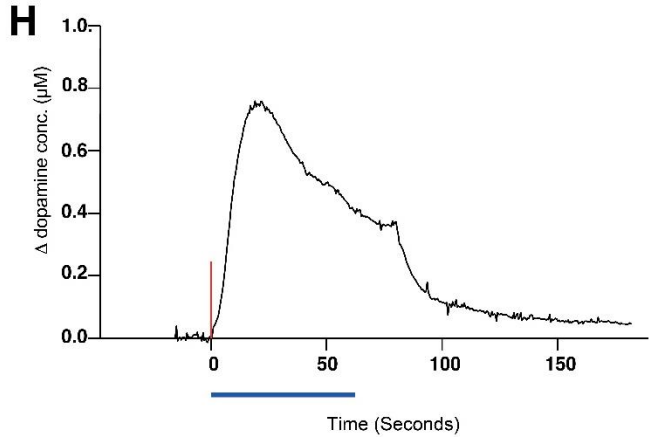

Figure 4 Grafted TH:Cre neurons respond to optogenetic light modulation. Representative whole-cell recordings of TH:Cre grafted cell in the striatum in current clamp mode stimulated by (**A**) negative and positive 25 pA-75 pA current injections, (**B**) 500 ms constant light stimulation (*blue line*), (**C**) light pulses at 10 Hz (*blue bars*), (**D**) light pulses at 20 Hz (*blue bars*), (**E**) 30 sec light off followed by 30 sec constant light (*blue line*). (**F-G^{I}**) Biocytin staining showing cell bodies and axonal extensions of patched grafted neurons in the striatum. (**H**) Representative trace of measured dopamine concentration (µM) from chronoamperometric recording in transplant with 60 sec light stimulation.

DISCUSSION

In the current study, we provide evidence on the application of optogenetics to dissect the functional integration of intracerebrally engrafted dopamine neurons in a preclinical animal model of PD. First, immunohistochemical analysis of TH:Cre cells transduced with AAV-ChR2-EYFP showed that the opsin can be selectively expressed in the TH- and Cre-positive cells. This suggested that optogenetic modulation of these cells would be possible to detect the dopamine release in real-time. Chronoamperometric recordings combined with laser stimulation validated this hypothesis and demonstrated, although not significant, increasing release trends of dopamine with higher constant laser intensities and stimulation duration. Furthermore, immunohistochemical and behavioural assessment of 6-OHDA-lesioned rats that were transplanted with TH:Cre derived progenitor cells showed complete depletion of dopamine with partial restoration after the transplant. Subsequently, the functioning of the neuronal graft was examined using optogenetic stimulation in an electrophysiological and electrochemical setting. This showed the ability of the graft to fire action potentials and to release dopamine, hence, proving the full maturation and activity of the transplanted cells.

Although GFP expression was validated and selective for TH:Cre cells, the level of viral infiltration seemed limited as not all TH:Cre-positive cells were expressing the transgene of interest. Enhancing the AAV transduction remains a common hurdle in the field that needs to be overcome (30-35). One of the main factors that needs to be considered is the AAV tropism, which is dominated by the AAV capsid proteins, as each AAV serotype targets slightly different cell populations (36). Whereas we use an AAV6 serotype in this study, the AAV1, AAV2, AAV5, AAV8, and AAV9 serotypes are more commonly used to target neurons, oligodendrocytes, and astrocytes (37-44). In particular, AAV2 capsids are known to have a high tropism for TH-positive dopamine neurons and a rather confined spread (45-47). This enables precise and local transduction and makes them appropriate for optogenetics. Also, the route of administration is an essential aspect to consider; however, by directly injecting the virus into the midbrain, we bypass the risk of triggering an immune response (48). Moreover, this provides the advantage of spatial targeting. Lastly, increased viral titres and dosages can be administered in order to improve the efficiency of viral transduction, yet, it has been reported adversely to induce toxicity (49, 50). Since AAVs transduce non-dividing cells such as neurons and have a minimal pathogenic character, their use is preferred over lentiviral vectors (51). Moreover, the DIO-AAV is a well-established method to achieve high cell specificity in a certain neuronal subtype, including dopamine neurons, through Cre-recombinase expression (52).

Furthermore, we demonstrated the potential of optogenetics to elicit dopamine release in ChR2-transfected dopamine neurons via chronoamperometric detection. These results are in line with previous *in vivo* studies that utilise ChR2 to induce dopamine release from dopaminergic neurons (53, 54). Despite the development of various methods such as neuroimaging and microdialysis to analyse dopamine levels, real-time electrochemical detection maintains a higher temporal resolution (55-57). In addition, we showed that the responsiveness of dopamine release alters when we use different stimulation parameters. Whereas constant light illumination suggests higher dopamine release compared to pulsed light, others have reported that frequency-based dopamine release was more dominant (53, 56). Although constant illumination was able to reach similar concentrations of dopamine, it evoked the highest background in dopamine currents (56). However, several variables can account for these differences. Firstly, the biological features of the ChR2 proteins can cause unique frequency-based responses and can require continuous light illumination (58). Subsequently, based on the target in the brain and the positioning of the stimulation-detection assembly, the release patterns can change.

Moreover, our results indicate that differences in dopamine release can be observed between several dorsoventral positions when we use a laser power higher than 1.25 mW. Also Bass et al. reported that the required minimum laser intensity to induce dopamine release from ChR2-expressing dopamine neurons was 1 mW (53). This is in accordance with blue light penetration properties in the striatum (53, 59). Starting from 1 mW, laser powers up to 5 mW

are described as sufficient to induce a dopamine response, and as shown in this study, higher laser intensities result in increased trends of dopamine release. However, the detrimental effects of light-induced tissue damage, potentially leading to an altered neuronal function or even neuronal death, need to be considered (22). Higher intensities might cause heat generation that can permanently damage the cells and affect their excitability (60). A recently published theoretical model to probe the temperature-generated effects in optogenetic experiments, emphasised that commonly used laser intensities increased the temperature in surrounding tissue (61). To exclude this criterium, we ran MatLab computer simulations for light-induced heat and light penetration (unpublished data). This suggested that 5 mW might elicit a raise in temperature and that the possibility of inducing the same effect should be taken into account for 2.5 mW stimulation as well. Therefore, it is more prominent to implement shorter laser radiation for these parameters.

Data obtained from the grafted animals validated already established findings on the maturation and survival of the dopaminergic progenitor cells (9). Since this project focused on elucidating the integration of the graft functionality using optogenetics, the amount of injected cells was purposely small, hence, also the limited (co-) expression. The reason for the small graft was to target all the cells within reach of the laser and eventually modulate their activity. Assessment of the graft with the amphetamine-induced rotation test led to contralateral rotations due to dopamine restoration. This data shows that the amphetamine test correlates well with the 6-OHDA motor impairments and graft-induced recovery, thereby remaining the gold standard in the field (29, 62). The mechanism of the apomorphine test works differently. Due to denervation of the striatum, there is an upregulation of postsynaptic hypersensitive dopamine receptors which engender contralateral rotations (63). Graft placement decreases the supersensitivity locally around the site of transplantation. Since the graft in this study is not large enough, it is not able to reduce the number of hypersensitive receptors more widespread. Therefore, the amphetamine-induced rotation test is a more accurate approach in this study design. Despite the small graft, also the cylinder test proposed a significant improvement of the PD-like impairments post-transplantation.

Finally, the intra- and extracellular features of TH:Cre derived fetal progenitor cells were investigated using optogenetics. Also Steinbeck et al. attempted to investigate the functional integration by optogenetically silencing the grafts through the use of inhibitory opsins (17). This resulted in a suppressed pacemaker activity of the cells during light stimulation. We, on the other hand, demonstrated the ability of the grafts to elicit optogenetics-mediated action potentials by activating the cells. A constant light was able to evoke one action potential, whereas pulsed light resulted in the firing of several spikes. This data goes against the stimulation parameters tested in AAV-ChR2-injected TH:Cre rats. A recently published work described that the somatodendritic dopamine release from nigral dopaminergic neurons was not affected by action potentials but is rather calcium-dependent (64). This suggests that dopamine release does not necessarily have to correlate with neuronal firing rates (65). Besides the electrophysiological properties of the grafts, we successfully demonstrated a release of dopamine from the transplanted dopaminergic neurons. Previous work from Aldrin-Kirk and Heuer et al. already revealed the release of dopamine after selective activation of dopaminergic transplants using chemogenetics (26, 66). This method has the advantage of less-invasive modulation of a selected cell population due to the absence of an optical fibre that might perturbates the animal behaviour (67). However, optogenetics is a more reliable method for obtaining a higher degree of temporal resolution as well as reversible control. By using optogenetics, we are the first to selectively activate dopaminergic transplants in a 6-OHDA animal model. Collectively, this data validates the correlation between graft-induced behavioural recovery and the functional graft connectivity.

There are some limitations in this study that should be recognised. First, significance was difficult to obtain in most of our results due to small sample sizes. Also considering practical reasons such as a limited time-frame and COVID-19 circumstances, not all experiments could be completed. This latter mainly clarifies the lack of data points in electrochemistry recordings, both in TH:Cre rats

and the hemiparkinsonian rats. Therefore, it would be interesting to further confirm the graft functionality with larger sample sizes and alternative techniques which target the selective and reversible control of a transplant in a less-invasive manner. Then, the next step in monitoring the graft-to-host connectivity would be the application of optogenetics in freely-moving rats, interestingly, over a longer period of time. Another considerable matter would be the implementation of another animal model of PD. The neurotoxin-based rodent model used in this study does not include the progressive degeneration but targets a sudden and thorough depletion of dopamine. Additionally, it does not display any α-synuclein (α-syn) protein aggregation, which is another main pathological hallmark of PD (68). Previous observations in a number of advanced patients who received a transplantation of fetally-derived dopamine grafts indicated that within a fraction of the transplanted cells, inclusions of phosphorylated α-syn were formed (69-71). Hoban et al. recently succeeded to model the contingent appearance of α-syn pathology in human fetal tissue-derived grafts (72). The utilisation of such a novel and humanised preclinical PD model would be an essential concern when considering the potency of cell replacement therapy in the clinic.

By gaining access and experimental control over the transplanted cells, our ability to conduct more studies on the graft functionality will increase. Since optogenetics enables selective and reversible control over the neurons, we can show the underlying mechanism of graft integration and recovery rather than linking the post-mortem biology to the behaviour. In a long term, this might be valuable in a patient setting as it will allow the fine-tuning of the graft activity. E.g. if the treatment would require more dopamine, we could increase release, and vice versa, the graft could be silenced when dyskinesias occur. The possibility to adjust the therapy is a major advantage when compared to pharmacotherapies where control is a challenging subject.

CONCLUSION

In summary, our data describes the potential of optogenetics to selectively manipulate dopaminergic grafts in a preclinical rodent model of PD. We proved that ChR2-transfected nigral cells are able to release dopamine provided that optimised optogenetic stimulation parameters are used. Besides, transplantation of dopaminergic progenitor cells in a 6-OHDA model, induced recovery from motor impairments. The graft-induced recovery was further confirmed by selectively activating the cells and measuring graft-specific intra- and extracellular properties. These results directly correlate the behavioural findings on recovery with the graft functionality. This evidence on the mechanism of neuronal network repair and the possibility of graft control strongly encourages cell replacement therapy towards treating PD.

Acknowledgements - I am grateful for Hasselt University (Belgium) and Prof. dr. Ilse Dewachter, coordinator of the course senior internship and the master subdivision, for arranging the internship program. I would also like to express my special thanks of gratitude to my promoter and supervisor Asst. Prof. Andreas Heuer for his valuable guidance and for giving me the opportunity to perform an internship in the Behavioural Neuroscience Laboratory (BNL) at the Biomedical Centre of Lund University (Sweden). I also want to thank dr. Francesco Gubinelli, Matilde Negrini, and all the members of the BNL for their limitless support and kindness during this internship. The advice and suggestions from this research group has had a major contribution to the laboratory and research skills that I have acquired as well as the manuscript that I have written. I would also like to express my special thanks of gratitude to my institutional promoter and supervisor, Prof. dr. Esther Wolfs and second examiner Prof. dr. Tim Vanmierlo for their guidance, support, availability, and kindness during this journey. I have gained experience and knowledge during this internship as well as during the master's program, for which I am very grateful.

Author contributions – AH designed the study and is the principal investigator. TB kindly provided access to the transgenic TH:Cre colony of animals. MD and MN produced the viruses used for this study. AH and FG performed all the surgeries. AH, FG, MN, and NC conducted all the *in vivo* experiments. NC performed all the immunohistochemistry stainings. ML performed the patch clamp recordings. AH, FG, and NC

analysed all the data. NC wrote the manuscript. AH, EW and FG supervised the internship. AH performed critical reading and provided feedback on the manuscript.

REFERENCES

1. Sherer TB, Chowdhury S, Peabody K, Brooks DW. Overcoming obstacles in Parkinson's disease. Mov Disord. 2012;27(13):1606-11.

2. Lanciego JL, Luquin N, Obeso JA. Functional neuroanatomy of the basal ganglia. Cold Spring Harb Perspect Med. 2012;2(12):a009621.

3. Struzyna LA, Browne KD, Brodnik ZD, Burrell JC, Harris JP, Chen HI, et al. Tissue engineered nigrostriatal pathway for treatment of Parkinson's disease. J Tissue Eng Regen Med. 2018;12(7):1702-16.

4. Pinder RM. Possible dopamine derivatives capable of crossing the blood-brain barrier in relation to Parkinsonism. Nature. 1970;228(5269):358.

5. Thanvi B, Lo N, Robinson T. Levodopa-induced dyskinesia in Parkinson's disease: clinical features, pathogenesis, prevention and treatment. Postgrad Med J. 2007;83(980):384-8.

6. Jankovic J, Aguilar LG. Current approaches to the treatment of Parkinson's disease. Neuropsychiatr Dis Treat. 2008;4(4):743-57.

7. Groiss SJ, Wojtecki L, Sudmeyer M, Schnitzler A. Deep brain stimulation in Parkinson's disease. Ther Adv Neurol Disord. 2009;2(6):20-8.

8. Barker RA, Drouin-Ouellet J, Parmar M. Cell-based therapies for Parkinson disease-past insights and future potential. Nat Rev Neurol. 2015;11(9):492-503.

9. Parmar M. Towards stem cell based therapies for Parkinson's disease. Development. 2018;145(1).

10. Grealish S, Diguet E, Kirkeby A, Mattsson B, Heuer A, Bramoulle Y, et al. Human ESC-derived dopamine neurons show similar preclinical efficacy and potency to fetal neurons when grafted in a rat model of Parkinson's disease. Cell Stem Cell. 2014;15(5):653-65.

11. Kirkeby A, Nolbrant S, Tiklova K, Heuer A, Kee N, Cardoso T, et al. Predictive Markers Guide Differentiation to Improve Graft Outcome in Clinical Translation of hESC-Based Therapy for Parkinson's Disease. Cell Stem Cell. 2017;20(1):135-48.

12. Kirkeby A, Grealish S, Wolf DA, Nelander J, Wood J, Lundblad M, et al. Generation of regionally specified neural progenitors and functional neurons from human embryonic stem cells under defined conditions. Cell Rep. 2012;1(6):703-14.

13. Kriks S, Shim JW, Piao J, Ganat YM, Wakeman DR, Xie Z, et al. Dopamine neurons derived from human ES cells efficiently engraft in animal models of Parkinson's disease. Nature. 2011;480(7378):547-51.

14. Barker RA, Parmar M, Studer L, Takahashi J. Human Trials of Stem Cell-Derived Dopamine Neurons for Parkinson's Disease: Dawn of a New Era. Cell Stem Cell. 2017;21(5):569-73.

15. Bjorklund A, Dunnett SB, Stenevi U, Lewis ME, Iversen SD. Reinnervation of the denervated striatum by substantia nigra transplants: functional consequences as revealed by pharmacological and sensorimotor testing. Brain Res. 1980;199(2):307-33.

16. Dunnett SB, Hernandez TD, Summerfield A, Jones GH, Arbuthnott G. Graft-derived recovery from 6-OHDA lesions: specificity of ventral mesencephalic graft tissues. Exp Brain Res. 1988;71(2):411-24.

17. Steinbeck JA, Choi SJ, Mrejeru A, Ganat Y, Deisseroth K, Sulzer D, et al. Optogenetics enables functional analysis of human embryonic stem cell-derived grafts in a Parkinson's disease model. Nat Biotechnol. 2015;33(2):204-9.

18. Duebel J, Marazova K, Sahel JA. Optogenetics. Curr Opin Ophthalmol. 2015;26(3):226-32.

19. Guru A, Post RJ, Ho YY, Warden MR. Making Sense of Optogenetics. Int J Neuropsychopharmacol. 2015;18(11):pyv079.

20. Mahmoudi P, Veladi H, Pakdel FG. Optogenetics, Tools and Applications in Neurobiology. J Med Signals Sens. 2017;7(2):71-9.

21. Stauffer WR, Lak A, Yang A, Borel M, Paulsen O, Boyden ES, et al. Dopamine Neuron-Specific Optogenetic Stimulation in Rhesus Macaques. Cell. 2016;166(6):1564-71 e6.

22. Yizhar O, Fenno LE, Davidson TJ, Mogri M, Deisseroth K. Optogenetics in neural systems. Neuron. 2011;71(1):9-34.

23. Kravitz AV, Freeze BS, Parker PR, Kay K, Thwin MT, Deisseroth K, et al. Regulation of parkinsonian motor behaviours by optogenetic control of basal ganglia circuitry. Nature. 2010;466(7306):622-6.

24. Zolotukhin S, Potter M, Zolotukhin I, Sakai Y, Loiler S, Fraites TJ, Jr., et al. Production and purification of serotype 1, 2, and 5 recombinant adeno-associated viral vectors. Methods. 2002;28(2):158-67.

25. Nolbrant S, Heuer A, Parmar M, Kirkeby A. Generation of high-purity human ventral midbrain dopaminergic progenitors for in vitro maturation and intracerebral transplantation. Nat Protoc. 2017;12(9):1962-79.

26. Aldrin-Kirk P, Heuer A, Wang G, Mattsson B, Lundblad M, Parmar M, et al. DREADD Modulation of Transplanted DA Neurons Reveals a Novel Parkinsonian Dyskinesia Mechanism Mediated by the Serotonin 5-HT6 Receptor. Neuron. 2016;90(5):955-68.

27. Heuer A, Lelos MJ, Kelly CM, Torres EM, Dunnett SB. Dopamine-rich grafts alleviate deficits in contralateral response space induced by extensive dopamine depletion in rats. Exp Neurol. 2013;247:485-95.

28. Dunnett S.B., Torres E.M. (2011) Rotation in the 6-OHDA-Lesioned Rat. In: Lane E., Dunnett S. (eds) Animal Models of Movement Disorders. Neuromethods, vol 61. Humana Press. https://doi.org/10.1007/978-1-61779-298-4_15.

29. Bjorklund A, Dunnett SB. The Amphetamine Induced Rotation Test: A Re-Assessment of Its Use as a Tool to Monitor Motor Impairment and Functional Recovery in Rodent Models of Parkinson's Disease. J Parkinsons Dis. 2019;9(1):17-29.

30. Bartus RT, Herzog CD, Chu Y, Wilson A, Brown L, Siffert J, et al. Bioactivity of AAV2-neurturin gene therapy (CERE-120): differences between Parkinson's disease and nonhuman primate brains. Mov Disord. 2011;26(1):27-36.

31. Bartlett JS, Kleinschmidt J, Boucher RC, Samulski RJ. Targeted adeno-associated virus vector transduction of nonpermissive cells mediated by a bispecific F(ab'gamma)2 antibody. Nat Biotechnol. 1999;17(2):181-6.

32. Muller OJ, Kaul F, Weitzman MD, Pasqualini R, Arap W, Kleinschmidt JA, et al. Random peptide libraries displayed on adeno-associated virus to select for targeted gene therapy vectors. Nat Biotechnol. 2003;21(9):1040-6.

33. Grimm D, Lee JS, Wang L, Desai T, Akache B, Storm TA, et al. In vitro and in vivo gene therapy vector evolution via multispecies interbreeding and retargeting of adeno-associated viruses. J Virol. 2008;82(12):5887-911.

34. Lisowski L, Dane AP, Chu K, Zhang Y, Cunningham SC, Wilson EM, et al. Selection and evaluation of clinically relevant AAV variants in a xenograft liver model. Nature. 2014;506(7488):382-6.

35. Maheshri N, Koerber JT, Kaspar BK, Schaffer DV. Directed evolution of adeno-associated virus yields enhanced gene delivery vectors. Nat Biotechnol. 2006;24(2):198-204.

36. Haery L, Deverman BE, Matho KS, Cetin A, Woodard K, Cepko C, et al. Adeno-Associated Virus Technologies and Methods for Targeted Neuronal Manipulation. Front Neuroanat. 2019;13:93.

37. Dodiya HB, Bjorklund T, Stansell J, 3rd, Mandel RJ, Kirik D, Kordower JH. Differential transduction following basal ganglia administration of distinct pseudotyped AAV capsid serotypes in nonhuman primates. Mol Ther. 2010;18(3):579-87.

38. Burger C, Gorbatyuk OS, Velardo MJ, Peden CS, Williams P, Zolotukhin S, et al. Recombinant AAV viral vectors pseudotyped with viral capsids from serotypes 1, 2, and 5 display differential efficiency and cell tropism after delivery to different regions of the central nervous system. Mol Ther. 2004;10(2):302-17.

39. Hadaczek P, Forsayeth J, Mirek H, Munson K, Bringas J, Pivirotto P, et al. Transduction of nonhuman primate brain with adeno-associated virus serotype 1: vector trafficking and immune response. Hum Gene Ther. 2009;20(3):225-37.

40. Hammond SL, Leek AN, Richman EH, Tjalkens RB. Cellular selectivity of AAV serotypes for gene delivery in neurons and astrocytes by neonatal intracerebroventricular injection. PLoS One. 2017;12(12):e0188830.

41. Masamizu Y, Okada T, Ishibashi H, Takeda S, Yuasa S, Nakahara K. Efficient gene transfer into neurons in monkey brain by adeno-associated virus 8. Neuroreport. 2010;21(6):447-51.

42. Masamizu Y, Okada T, Kawasaki K, Ishibashi H, Yuasa S, Takeda S, et al. Local and retrograde gene transfer into primate neuronal pathways via adeno-associated virus serotype 8 and 9. Neuroscience. 2011;193:249-58.

43. Taymans JM, Vandenberghe LH, Haute CV, Thiry I, Deroose CM, Mortelmans L, et al. Comparative analysis of adeno-associated viral vector serotypes 1, 2, 5, 7, and 8 in mouse brain. Hum Gene Ther. 2007;18(3):195-206.

44. von Jonquieres G, Mersmann N, Klugmann CB, Harasta AE, Lutz B, Teahan O, et al. Glial promoter selectivity following AAV-delivery to the immature brain. PLoS One. 2013;8(6):e65646.

45. Castle MJ, Turunen HT, Vandenberghe LH, Wolfe JH. Controlling AAV Tropism in the Nervous System with Natural and Engineered Capsids. Methods Mol Biol. 2016;1382:133-49.

46. Koprich JB, Johnston TH, Reyes MG, Sun X, Brotchie JM. Expression of human A53T alpha-synuclein in the rat substantia nigra using a novel AAV1/2 vector produces a rapidly evolving pathology with protein aggregation, dystrophic neurite architecture and nigrostriatal degeneration with potential to model the pathology of Parkinson's disease. Mol Neurodegener. 2010;5:43.

47. Watakabe A, Ohtsuka M, Kinoshita M, Takaji M, Isa K, Mizukami H, et al. Comparative analyses of adeno-associated viral vector serotypes 1, 2, 5, 8 and 9 in marmoset, mouse and macaque cerebral cortex. Neurosci Res. 2015;93:144-57.

48. Colella P, Ronzitti G, Mingozzi F. Emerging Issues in AAV-Mediated In Vivo Gene Therapy. Mol Ther Methods Clin Dev. 2018;8:87-104.

49. Hinderer C, Bell P, Vite CH, Louboutin JP, Grant R, Bote E, et al. Widespread gene transfer in the central nervous system of cynomolgus macaques following delivery of AAV9 into the cisterna magna. Mol Ther Methods Clin Dev. 2014;1:14051.

50. Lavin TK, Jin L, Lea NE, Wickersham IR. Monosynaptic Tracing Success Depends Critically on Helper Virus Concentrations. Front Synaptic Neurosci. 2020;12:6.

51. Mei Y, Zhang F. Molecular tools and approaches for optogenetics. Biol Psychiatry. 2012;71(12):1033-8.
52. Smedemark-Margulies N, Trapani JG. Tools, methods, and applications for optophysiology in neuroscience. Front Mol Neurosci. 2013;6:18.
53. Bass CE, Grinevich VP, Vance ZB, Sullivan RP, Bonin KD, Budygin EA. Optogenetic control of striatal dopamine release in rats. J Neurochem. 2010;114(5):1344-52.
54. Tsai HC, Zhang F, Adamantidis A, Stuber GD, Bonci A, de Lecea L, et al. Phasic firing in dopaminergic neurons is sufficient for behavioral conditioning. Science. 2009;324(5930):1080-4.
55. Bazzu G, Calia G, Puggioni G, Spissu Y, Rocchitta G, Debetto P, et al. alpha-Synuclein- and MPTP-generated rodent models of Parkinson's disease and the study of extracellular striatal dopamine dynamics: a microdialysis approach. CNS Neurol Disord Drug Targets. 2010;9(4):482-90.
56. Chiu WT, Lin CM, Tsai TC, Wu CW, Tsai CL, Lin SH, et al. Real-time electrochemical recording of dopamine release under optogenetic stimulation. PLoS One. 2014;9(2):e89293.
57. Meyer JH. Neuroimaging markers of cellular function in major depressive disorder: implications for therapeutics, personalized medicine, and prevention. Clin Pharmacol Ther. 2012;91(2):201-14.
58. Deisseroth K, Hegemann P. The form and function of channelrhodopsin. Science. 2017;357(6356).
59. Gradinaru V, Mogri M, Thompson KR, Henderson JM, Deisseroth K. Optical deconstruction of parkinsonian neural circuitry. Science. 2009;324(5925):354-9.
60. Stujenske JM, Spellman T, Gordon JA. Modeling the Spatiotemporal Dynamics of Light and Heat Propagation for In Vivo Optogenetics. Cell Rep. 2015;12(3):525-34.
61. Peixoto HM, Cruz RMS, Moulin TC, Leao RN. Modeling the Effect of Temperature on Membrane Response of Light Stimulation in Optogenetically-Targeted Neurons. Front Comput Neurosci. 2020;14:5.
62. Ungerstedt U. Striatal dopamine release after amphetamine or nerve degeneration revealed by rotational behaviour. Acta Physiol Scand Suppl. 1971;367:49-68.
63. Ungerstedt U. Postsynaptic supersensitivity after 6-hydroxy-dopamine induced degeneration of the nigro-striatal dopamine system. Acta Physiol Scand Suppl. 1971;367:69-93.
64. Yee AG, Forbes B, Cheung PY, Martini A, Burrell MH, Freestone PS, et al. Action potential and calcium dependence of tonic somatodendritic dopamine release in the Substantia Nigra pars compacta. J Neurochem. 2019;148(4):462-79.
65. Liu C, Kaeser PS. Mechanisms and regulation of dopamine release. Curr Opin Neurobiol. 2019;57:46-53.
66. Aldrin-Kirk P, Heuer A, Rylander Ottosson D, Davidsson M, Mattsson B, Bjorklund T. Chemogenetic modulation of cholinergic interneurons reveals their regulating role on the direct and indirect output pathways from the striatum. Neurobiol Dis. 2018;109(Pt A):148-62.
67. Vlasov K, Van Dort CJ, Solt K. Optogenetics and Chemogenetics. Methods Enzymol. 2018;603:181-96.
68. Braak H, Braak E. Pathoanatomy of Parkinson's disease. J Neurol. 2000;247 Suppl 2:II3-10.
69. Li JY, Englund E, Holton JL, Soulet D, Hagell P, Lees AJ, et al. Lewy bodies in grafted neurons in subjects with Parkinson's disease suggest host-to-graft disease propagation. Nat Med. 2008;14(5):501-3.
70. Li JY, Englund E, Widner H, Rehncrona S, Bjorklund A, Lindvall O, et al. Characterization of Lewy body pathology in 12- and 16-year-old intrastriatal mesencephalic grafts surviving in a patient with Parkinson's disease. Mov Disord. 2010;25(8):1091-6.
71. Li W, Englund E, Widner H, Mattsson B, van Westen D, Latt J, et al. Extensive graft-derived dopaminergic innervation is maintained 24 years after transplantation in the degenerating parkinsonian brain. Proc Natl Acad Sci U S A. 2016;113(23):6544-9.
72. Hoban DB, Shrigley S, Mattsson B, Breger LS, Jarl U, Cardoso T, et al. Impact of alpha-synuclein pathology on transplanted hESC-derived dopaminergic neurons in a humanized alpha-synuclein rat model of PD. Proc Natl Acad Sci U S A. 2020;117(26):15209-20.

SUPPLEMENTARY INFORMATION

Supplementary methods

Preparation of fetal dopaminergic grafts

Male TH:Cre homozygote Sprague-Dawley rats were time-mated with female wild type Sprague-Dawley rats. At E14, the embryonic sacs were removed and transferred to ice-cold DMEM/F12 media (Gibco, Life Technologies). The ventral mesencephalon was carefully dissected from each fetus and collected in ice-cold DMEM/F12 media. Afterwards, the culture media was removed and the cell suspension was incubated with 0,1 % trypsin (Gibco, Life Technologies) and 0,05 % DNAse (Qiagen) in HBSS (Gibco, Life Technologies) for 20 min at 37° C. The trypsin solution was washed away (3x) and replaced with HBSS/DNAse solution. Following, cells were dissociated by mechanically pipetting until the solution became cloudy and homogeneous. The cells were then centrifuged at 600 g for 5 min and re-suspended in HBSS/DNAse. The cell count/ viability was quantified using trypan blue and the cell concentration was diluted to 10E4 viable cells/µl. Wild type Sprague-Dawley rats with 6-OHDA lesions received a total of 200 000 cells into the striatum.

Immunohistochemistry

Sections were washed (3x) in phosphate buffered saline with potassium (KPBS) and then quenched for 15 min followed by washing steps with KPBS (3x) and blocking in 5% serum in TXTBS (KPBS + 0.2% Triton X-100, pH=7.4) for 1 h. Sections were then incubated in primary antibody in 5% serum overnight at room temperature (**Suppl. Table 1**). The primary antibody was washed away (2x) using KPBS and incubated for 20 min in 5% serum. The sections were then incubated in a secondary antibody solution in 5% serum for 1 h followed by KPBS washing steps (3x). For 3, 30-diaminobenzidine (DAB) immunohistochemistry, the sections were incubated in avidin-biotin based ABC solution (Vectorlabs) for 1 h to amplify the staining intensity. The sections were washed in KPBS (3x) and were incubated for 2 min in DAB solution. The brain sections were then mounted on gelatin-coated glass slides and dehydrated through incubation in a series of increasing ethanol concentrations followed by Xylene incubation and coverslipping using DPX. For Fluorescent staining, the quenching step was excluded and the sections were incubated in fluorophore-conjugated secondary antibodies. PVA-DABCO was used as the mounting medium. For immunostaining against biocytin, the slices were washed with KPBS (3x) and incubated in TXTBS blocking solution for 1 h. The sections were then incubated with Alexa 647-conjugated streptavidin (1:1000, Invitrogen) in 5% blocking solution and washed with KPBS (3x). Slides were cover-slipped with Vectashield (Vector Laboratories) and sealed with nail polish.

Supplementary Table 1 Used primary and secondary antibodies for immunohistochemical analysis

1° AB	Species	Cat. no.	Conc. 1°	Serum	2° AB	Cat. no.	Conc. 2°
GFP	Chicken	A10262 (Thermofisher)	1:1000	Goat	Anti-chicken	BA9010 (Vector)	1:200
GFP	Chicken	A10262 (Thermofisher)	1:1000	Goat	Anti-chicken	Alexa 488 (Invitrogen)	1:500
TH	Rabbit	AB152 (Sigma-Aldrich)	1:1000	Goat	Anti-rabbit	Alexa 568 (Invitrogen)	1:500
Cre	Mouse	AB24607 (Abcam)	1:500	Donkey	Anti-mouse	Alexa 647 (Invitrogen)	1:500
TH	Rabbit	AB152 (Sigma-Aldrich)	1:1000	Goat	Anti-rabbit	BA1000 (Vector)	1:200

In vivo electrochemistry

Chronoamperometric recordings of dopamine release in the striatum were performed as previously described (26). A square wave-potential (+0.55 V; resting 0 V vs an Ag/AgCl reference electrode) was

applied and oxidation/reduction currents were recorded with Nafion-coated (Sigma Aldrich) carbon fibre electrodes (diameter 20-30 µm; length 100-150 µm) (Quanteon, KY, US) using a Pentium-IV microcomputer-controlled instrument (FAST-16; Quanteon). Prior to recording, each electrode was calibrated in 0.1 M PBS (pH=7.4) and only the electrodes that showed a linear response rate to three additions of 2 µM dopamine ($r^2 < 0.995$), a selectivity ratio of dopamine to ascorbic acid greater than 100:1 with a limit of detection smaller than 0.1 were used. Using stick wax, the calibrated electrode was assembled together with a pulled glass capillary and an optical fibre (numerical aperture 0.39, 200 µm core diameter, Thorlabs) with an average distance of 100 µm between each of them. Light stimulation was monitored using the Master-8 pulse generator (AMPI). The glass capillary was filled with KCl (120 mM, pH=7.4) to stimulate dopamine release and connected to a picospritzer (Aldax) micropressure system. Meanwhile, an Ag wire was electroplated in 1 M HCl solution saturated with NaCl for at least 20 min to be used as Ag/AgCl reference electrode. For the recording, anaesthetised rats (1.5-3% isoflurane) were head fixed into the stereotactic frame. The assembly was descended into the brain at AP: +0.5; ML: -2.0; DV: -1.0/-3.5/-4.5/-5.5 and the reference electrode was placed under the skin. The electrode was allowed to calibrate and reach a baseline before recordings started. Three successive recordings were performed for each stimulation parameter, shown in Table 2. Recordings typically lasted between 6-10 h.

Whole-cell patch-clamp electrophysiology

Slices were individually placed in a dual-flow recording chamber and held in place using a horseshoe shaped flattened platinum wire. The slices were constantly perfused with oxygenated aCSF fluid in which the temperature was maintained at 32–34°C. The GFP-positive cells in the engrafted striatum were visualised using fluorescent light and they were approached by the recording pipette using infrared differential interference contrast microscopy. Recording pipettes (tip resistance 2.5-6 MΩ) were pulled from borosilicate glass with a Flaming-Brown horizontal puller (P-97, Sutter Instruments, Novato, CA, USA), and were filled with patch solution. Pipettes were connected to a HEKA amplifier (HEKA, Germany) controlled with HEKA Patchmaster software. Whole-cell current clamp recordings were performed using a Multiclamp 700B amplifier (Molecular Devices) after formation of a Giga-seal by rupturing the patch. The firing activity of the cells was recorded by injecting a 100 ms square pulse of 25-75 pA. Light-induced recordings were based on single 500 ms constant, 1 ms at 10 Hz frequency, 1 ms at 20 Hz frequency, or 30 sec constant off-on light pulses. After recording, biocytin was allowed to diffuse in the cell during 10 min.

Composition of used buffers and solutions

6-OHDA 14 µg free base in ascorbate-saline (0.02%) injected at a concentration of 3.5 µg/µl
Antifreeze solution 0.5M sodium phosphate buffer, 30% glycerol and 30% ethylene glycol
Quench 10% H_2O_2, 10% Methanol, 80% KPBS
Sucrose based cutting solution sucrose 75 mM, NaCl 67 mM, NaHCO3 26 mM, glucose 25 mM, KCl 2.5 mM, NaH2PO4 1.25 mM, CaCl2 0.5 mM, MgCl2 7 mM, pH 7.4, osmolarity 305–310 mOsm
aCSF NaCl 119 mM, NaHCO3 26 mM, glucose 25 mM, KCl 2.5 mM, NaH2PO4 1.25 mM, CaCl2 2.5 mM and MgSO4 1.3 mM, pH 7.4, osmolarity 305–310 mOsm)
Patching solution K-gluconate 122.5 mM, KCl 12.5 mM, KOH-HEPES 10 mM, KOH-EGTA 0.2 mM, MgATP 2 mM, Na3GTP 0.3 mM, NaCl 8 mM (pH 7.2–7.4, mOsm 300–310) and 0.5% biocytin

Supplementary figures

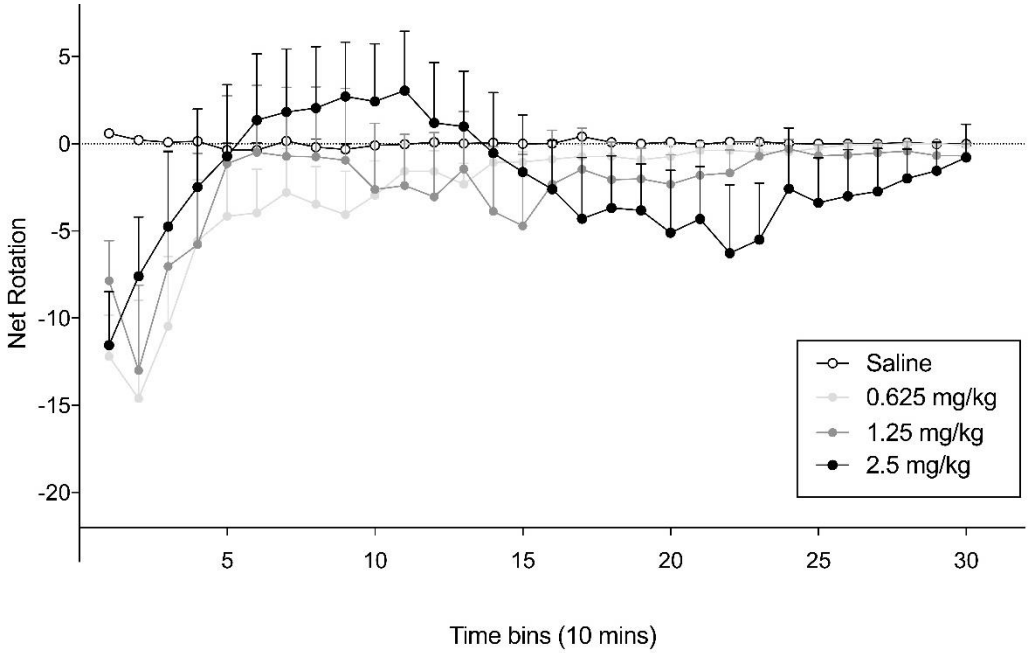

Supplementary Figure 1 Amphetamine-induced rotation test with different injected concentrations over a 300 min time course to show that low concentrations of amphetamine injections are only able to stimulate the grafted hemisphere. 6-OHDA animals (*lesioned in right hemisphere*) showing the most successful lesions (n=5) were selected, post-transplantation with fetal TH:Cre-derived dopaminergic cells, for four repetitions of the drug-induced rotation test over a 300 min testing period with a different injected concentration for each test. Rats displayed a quiet baseline activity after saline injection. Injection with 0.625 mg/kg demonstrated a net contralateral rotation in the first 50 min, indicating a graft maturation, followed by a direct return to the baseline. Injection with 1.25 mg/kg amphetamine showed an initial contralateral rotation due to a successful graft followed by a shift to ipsilateral rotations between min 50 and 100, indicating that this amphetamine concentration was able to also induce a rotational effect from the unaffected hemisphere. Rats displayed an initial contralateral rotational behaviour after 2.5 mg/kg amphetamine injection due to graft maturation. Then the rats reached a peak of ipsilateral rotations around min 100, indicating that the highest dose of amphetamine stimulated the unaffected hemisphere to initiate ipsilateral rotations. This was followed by a lower peak of contralateral rotations around min 200 due to take-over of the grafted hemisphere.